RSC Advances

PAPER

View Article Online
View Journal | View Issue

Check for updates

Cite this: *RSC Adv.*, 2026, **16**, 23715

Encapsulated essential oil-based nanoemulsion beads: a green innovation for storage pest control against *Tribolium castaneum*

Nagarathinam Kannan [a] and Natarajan Chandrasekaran *[b]

Essential oil nanoemulsion formulations offer environmentally friendly, safer alternatives to synthetic insecticides for integrated pest management, thereby reducing food loss and financial losses caused by the infestations of pests like *Tribolium castaneum*. In order to manage the infestations caused by *Tribolium castaneum*, we formulated nanoemulsion beads with cinnamon and clove essential oils and purified eugenol. Initially, we formulated the nanoemulsion beads with sodium alginate, characterized the formulations, and investigated their properties for repellent, ovicidal, fumigant and larvicidal activities against *T. castaneum* to analyze the efficacy of the essential oils. Characterization analysis showcased the formulated NE bead size of 1.34 mm and surface characterization showed the adsorption–desorption isotherms, revealing the porous structure. Moreover, FT-IR spectroscopy and GC-MS analysis showed the presence of essential oils in the formulated beads. Further, *in vitro* analysis revealed the CNN excellence in the fumigant activity, showcasing the highest mortality rate of approximately 8% at the highest time point of 36 h exposure. Nevertheless, it also excelled in the ovicidal and larvicidal activities. Cinnamon NE beads showed highest mortality rate at 98 h and 30 h time point respectively, followed by EGN and CLN beads. Meanwhile, in all *in vitro* assessments, the control sodium alginate beads showed no effect, indicating that its presence does not impact *Tribolium castaneum*. Based on these *in vitro* assessment results, it is evident that the Cinnamon NEs beads have significant effect on the treating *Tribolium castaneum*, also proving the formulated NEs beads with sodium alginate doesn't infer in the any toxic effect against the insects. In conclusion, the study depicts that the development of nanoemulsion beads of the essential oils improved their stability compared with nanoemulsions. Moreover, essential oils enhanced the efficacy of the beads, paving the way for reduced use of harmful synthetic insecticides and pesticides against the stored grain pests.

Received 23rd March 2026
Accepted 6th April 2026

DOI: 10.1039/d6ra02377k

rsc.li/rsc-advances

Open Access Article. Published on 06 May 2026. Downloaded on 6/2/2026 7:40:05 AM.
This article is licensed under a Creative Commons Attribution-NonCommercial 3.0 Unported Licence.

1. Introduction

The global population growth rate of 1.5% poses a significant challenge to food grain delivery, which accounts for 67–80% of the human food supply, while pests cause severe damage to stored food grains.[1] The infestations of pests, such as the red flour beetle, cause significant food loss during storage, leading to financial losses in both developed and developing countries.[2,3] Significant economic losses and quality deterioration occur mainly due to *Tribolium castaneum*, commonly known as the red flour beetle, and hence, it is necessary to control this pest in stored grains like wheat flour.[4] About 10–15% wheat, a major cereal crop, is lost annually due to stored grain pests, primarily the red flour beetle, *Tribolium castaneum*, which is a serious and cosmopolitan issue.[5] Nowadays, essential oils provide a potent, natural, and sustainable solution for managing *T. castaneum* due to their effectiveness, eco-friendliness, and sustainable pest management contribution. In case of high insecticidal activity, essential oils such as cinnamon and clove oils have demonstrated very high activity against both adult and immature stages of *T. castaneum*.[6] Many essential oils also display significant repellent properties that reduce beetle infestation by preventing pest colonization and feeding.[7] Oils from peppermint, lavender, rose, and jasmine have shown both toxic and repellent activities against red flour beetles in direct contact and fumigation assays.[8] Moreover, essential oils negatively affect the reproductive cycle and development of *T. castaneum*, reducing their pupal formation and adult emergence, which helps to break the pest life cycle and lower population growth over time.[6] Stored-product insect pests have traditionally been controlled using chemical fumigants, mainly phosphine and methyl bromide, in bulk grains, warehouses, and commodity stores. Additionally, organophosphate and synthetic pyrethroid insecticides are applied as grain protectants and structural sprays to manage leftover

[a]*Department of Biotechnology, School of Biosciences and Technology, Vellore Institute of Technology, Vellore, Tamil Nadu, India*
[b]*Centre for Nanobiotechnology (CNBT), Vellore Institute of Technology, Vellore, Tamil Nadu, India. E-mail: nchandrasekaran@vit.ac.in*

© 2026 The Author(s). Published by the Royal Society of Chemistry

Open Access Article. Published on 06 May 2026. Downloaded on 6/2/2026 7:40:05 AM. This article is licensed under a Creative Commons Attribution-NonCommercial 3.0 Unported Licence.

infestations. In case of resistance development, intensively repeated use of phosphine has led to widespread resistance in major stored-product pests, causing control failures in several regions. Resistance to contact insecticides (organophosphates and pyrethroids) is also well documented, reducing the reliability of conventional programs.[9] Some key negative impacts of pesticide use include significant human health concerns, as toxic gases like phosphine and methyl bromide pose acute and chronic risks to workers and nearby individuals. Broader pesticide use has been linked to increased cancer risks and other health disorders in exposed populations. Environmentally, methyl bromide depletes the ozone layer and has been restricted globally, while other pesticides contribute to biodiversity loss.[7] Additionally, chemical residues from fumigants raise food safety issues, impacting trade and consumer acceptance, especially with stringent maximum residue limits.[10] While, regulatory pressures have led to stricter regulations and a decline in conventional insecticide use in postharvest systems. In order to overcome these issues, we developed a green approach of using essential oils for controlling stored grain pests. Key challenges include volatility, stability, and controlled release. In order to overcome these issues, advanced techniques are used in the formulation of essential oil nanosystems to improve their bioactivity and functionality across various applications.[11] Nanoemulsions efficiently transport active substances through a semipermeable membrane, increasing penetration and preventing droplet flocculation due to their large surface area and small globule size.[12] Nanoemulsions can be formulated to target specific life stages of the beetle, such as larvae or adults, by adjusting the formulation or using different essential oils.[13,14] Nanoemulsions can be more effective than traditional insecticides in controlling pest populations, offering a promising alternative for integrated pest management strategies.[15] Nanoemulsion formulations of essential oils have been studied as a novel, bio-rational, and effective approach to control the red flour beetle, especially *T. castaneum*, a significant pest of stored grain products. Several essential oils like chamomile, cumin, peppermint, anise, and clove have been formulated into nanoemulsions, which enhance the insecticidal efficacy, stability, and delivery of the oils.[16] These nanoemulsions show lethal and sublethal toxicities to the red flour beetle, impairing their feeding, reproduction, and survival, thus protecting stored grains from damage.[17] Clove oil nanoemulsions were highly toxic against beetles and larvae, with calculated LC50 values indicating strong efficacy at low concentrations.[18] The droplet sizes typically in the nanometer range (around 200–400 nm) improve solubility, diffusion, and insecticide delivery.[19,20] Nanoemulsion formulations offer environmentally friendly, safer alternatives to synthetic insecticides, suitable for integrated pest management programs targeting stored product pests like red flour beetle. Encapsulation technologies, like micro- and nano-encapsulation, address food grain storage, insect infestation, and nutrient loss. They prolong pesticide and insecticide activities, enhance grain safety, and promote sustainable agricultural practices, ensuring high-quality standards for food grains.[21] Nanoemulsion beads or formulations can effectively control pests in stored grains, such as red flour beetles and rice weevils, due to their extended biological activity and enhanced efficacy.[22] These nanoemulsions require lower active ingredient concentrations and have lower environmental toxicity. However, large-scale commercial adoption and long-term environmental impact assessments are still ongoing, necessitating further research and regulatory evaluations.[23] Based on the literature review, there is a research gap in formulating nanoemulsion beads as specific products for pest infestation, but typically these formulations involve oil-in-water nanoemulsions prepared by methods like ultrasonic emulsification with surfactants (*e.g.*, Tween 80) to stabilize the droplets. These formulations can be adapted into beads or granules for practical use. The literature suggests that nanoemulsion bead products, containing oil-in-water nanoemulsions, can effectively control red flour beetles in stored products by enhancing the efficacy, reducing dosages, and preserving grain quality, with potential as biopesticides in integrated pest management. Addressing this research gap, we formulated the nanoemulsion beads with the cinnamon essential oil, clove essential oil and purified eugenol for treating *T. castaneum*. Initially, we formulated the nanoemulsion beads with sodium alginate and carried out their characterization analysis using FESEM, Fourier transform infrared (FTIR) spectroscopy and GC-MS analysis. Then, the activity of the formulated nanoemulsion sodium alginate beads was tested for repellent, ovicidal, fumigant and larvicidal activities against *T. castaneum* to analyze the efficacy of the essential oils.

2. Materials and methods

2.1 Study location

The research was conducted from 2024 to 2025 at the School of Biosciences and Technology, Vellore Institute of Technology, Vellore, at the Centre for Nanotechnology Research Laboratory.

2.2 Insect rearing

Tribolium castaneum adult insects were purchased from the Indian Institute of Food Processing Technology, Thanjavur (IIFPT). We maintained the standard rearing procedures described in previous studies by Sokoloff, 1972 and Goodman *et al.*, 2012.[24,25] Insects were reared on sterile wheat flour under controlled laboratory conditions (an optimal temperature in the range of 25–30 °C and a relatively high humidity of about 70%). Each stage of insects was distinguished based on the literature (Mamata and Kumar (2021)).[26] A total of seven larval instars were identified and characterized as campodeiform and slender, with fine bristles on their dorsal surfaces. The colour and characteristics of each instar vary: the 1st instar is tiny and ivory white, the 2nd is mobile and linen white, the 3rd is thread-like and light yellowish, the 4th is light brownish, the 5th is immature and tortilla-coloured, the 6th is large and bulgy with a light brown colour, and the 7th is mobile and tawny. The pupal phase consists of three stages: pre-pupal (light yellowish, smaller, with fine bristles and shedding exuvia), pupal (darker, shorter, with hind limbs and small eyespots), and post pupal (fully developed eyes and hind limbs, dark brownish). Sexual

© 2026 The Author(s). Published by the Royal Society of Chemistry

Open Access Article. Published on 06 May 2026. Downloaded on 6/2/2026 7:40:05 AM. This article is licensed under a Creative Commons Attribution-NonCommercial 3.0 Unported Licence.

dimorphism is noted in pupae, with females having forked genital papillae longer than the stubby papillae of males. Adults are dark brownish, exhibiting sexual dimorphism with males having a setiferous patch on the forefemur, which is absent in females. Both adults feature prominent capitate antennae. In this study, we purchased adult insects and they were placed in sterile wheat flour, given a full day to oviposit to acquire synchronized developmental stages. Adults were carefully removed by sieve after this time to stop more egg laying. The same environmental conditions were used to incubate the obtained eggs. Larval age was measured from the day of hatching based on Mamata and Kumar's study (2021), with experiments conducted at this stage. Egg and larval stages were focused in this study, while individuals were monitored and handled under sterile conditions to reduce environmental variation.[27] Newly emerging individuals of both sexes were considered for this study.[28]

2.3 Chemical compounds

Eugenol (99% purity) and cinnamon leaf oil (Ceylon origin) (purity 99%) were acquired from Sigma-Aldrich (USA), and analytical grade methanol (99.8% purity) was purchased from S D Fine-Chem Limited (SDFCL) (Gujarat). Clove oil (99% purity) was purchased from SDFCL (Gujarat). We bought Tween 20 (polyethylene glycol sorbitan monolaurate) from Sigma-Aldrich (USA).

2.4 Preparation and characterization of nanoemulsions

Nanoemulsions (NEs) of the three essential oils, cinnamon, clove, and eugenol, were prepared using high-energy techniques, namely ultrasonication (150 W with 5, 10, and 15 minutes sonication) and homogenization (four different homogenization pressures, 5000, 10 000, 15 000, and 20 000 psi, for three different numbers of passes, 1, 2 and 3 times). Then, they are kept in opaque bottles at room temperature; in order to check the stability of the NEs for long-term storage, the samples were kept at 4 °C and 25 °C for 30 days. In order to prepare the NE beads, these essential oil nanoemulsion were initially added to the sodium alginate solution by stirring slowly. Then, this mixture is dropped into a calcium chloride solution, forming gel beads. These gel beads are allowed to harden for 20–30 minutes, followed by rinsing in distilled water and drying under controlled conditions.[29] For large-scale production of NE bead preparation, we used the novel bead encapsulator and dried the beads at 60 °C in a hot air oven. The bead sizes were measured using screw cage, and an average size of 100 beads were considered for this study. Regarding the characterisation of the oil nanoemulsion, field emission scanning electron microscopy (FESEM) analysis, GC-MS analysis, and Fourier-Transform Infrared (FTIR) Spectroscopy (JASCO) and gas chromatography analysis were carried out.[30]

2.4.1. Morphological analysis of the nanoemulsion beads. FESEM and EDX analyses were performed to provide comprehensive characterization of nanoemulsion beads by combining morphological imaging with their elemental composition analysis. This analysis was carried out in Prof. CNR Rao Research Centre at Avinashilingam Institute for Home Science and Higher Education, Coimbatore, Tamil Nadu.

2.4.2. Surface characterization of the nanoemulsion beads. BET analysis (Brunauer–Emmett–Teller analysis) was used to determine a surface area of the nanoemulsion beads, measuring the amount of gas adsorbed onto the surface under controlled conditions. BET analysis was performed in the Material Analysis and Research Centre (MARC material experts), Bangalore.

2.4.3. Chemical composition analysis of three essential oils. In order to analyse the chemical compositions in the NE beads, the beads are dissolved in 1 mL of methanol and incubated for 1 hour. Followed by centrifugation at 7000 rpm for 5 minutes, the supernatants are used for the GC-MS analysis. The NEs were analysed using an HP Agilent 6890 plus gas chromatograph (GC) fitted with an HP-5MS column (length: 30 m, internal diameter: 0.25 mm, and film thickness: 0.25 mm). After 8 minutes at 60 °C, the column temperature was increased to 250 °C at a rate of 2 °C per minute. The temperatures of the injector and detector were maintained at 250 °C and 270 °C, respectively. Helium served as the carrier gas, the column's flow rate was 0.5 mL min^{-1}, and 0.2 μL of oil sample was injected to set the split ratio to 5 : 1. We performed the GC/MS study using a quadrupole mass spectrometer operating at 70 eV. The area of the chromatographic peaks was used to calculate the content of NE compounds.[31]

2.4.4. Fourier-transform infrared (FT-IR) spectroscopy analysis. To identify the functional groups in each material utilized to create the NE beads, the beads were dissolved in 1 mL of methanol, incubated for 1 hour, and centrifuged at 7000 rpm for 5 minutes, and the supernatants were used for the FT-IR analysis. To investigate the interactions between them, Fourier transform infrared (FTIR) spectroscopy analysis was carried out. The samples were scanned in the 4000–500 cm^{-1} scanning range using an FTIR spectrophotometer (Jasco, India).[32,33]

2.5 *In vitro* studies for *Tribolium castaneum* using nanoemulsions

2.5.1. Evaluation of repellent activity. For this assay, the nanoemulsion beads were kept in the centre of the Petri dish. The smaller Petri plate of 50 × 12 mm size and the larger Petri plate of 90 × 15 mm size, as shown in Fig. 2, were used to check the repellent activity. Around 20 larvae were placed around the plate. Then, the whole Petri dish was closed, triplicates of the experiment were performed and the insects were observed for a maximum time period of 24 h. The numbers of larvae present in the treated and untreated zones were recorded. A graph was plotted using the recorded data of the number of larvae present in the treated zone as the percentage of repellent activity of the test solutions.[34,35]

2.5.2. Evaluation of fumigant activity. The fumigant activity of *T. castaneum* was evaluated using the following method. Briefly, the nanoemulsion beads (cinnamon oil nanoemulsion: CNN, clove oil nanoemulsion: CLN, and eugenol nanoemulsion: EGN) were added to the storage pest control device, as shown in Fig. 1. The caps were then screwed tightly

Open Access Article. Published on 06 May 2026. Downloaded on 6/2/2026 7:40:05 AM.
This article is licensed under a Creative Commons Attribution-NonCommercial 3.0 Unported Licence.

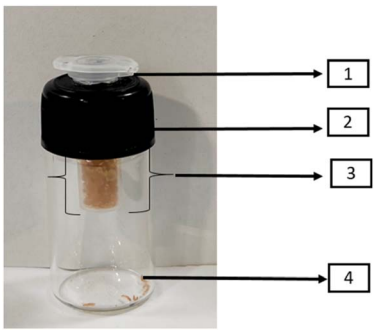

Fig. 1 Storage pest control device. (1) Sample box: the sample box contains a bio-pesticide which helps in the efficient release of the bio-pesticide into the storage box. The sample box capacity is 2 mL, which can store a liquid volume of 2 mL and a solid volume of 2 g of the bio-pesticide. The sample box contains a release outlet for releasing the bio-pesticide. The design for the storage pest control device was made of plastics. This sample box can be altered with stainless steel in future and is replaceable. Sample box is maintained in such a way without a contact with the stored products in the storage box. The upper side of the sample box is kept in an open-close manner like a door to load the bio-pesticides. (2) Sample box holder: this part holds the sample box containing the bio-pesticide. The diameter of the sample box holder is 10 mm. The sample box holder is air proof and ensures the non-leakage of the volatile products from the bio-pesticides. (3) Release outlet of sample box: the release outlet (holes) is kept in the sides of the sample box to ensure the efficient release of the bio-pesticide. Around 20 release outlets are kept in the 4 sides of the sample box. The diameter of the release outlets is 0.5 mm each. (4) Storage box: the storage box contains the stored food products along with the pests. This area is used for storing the food products. The storage box volume is 10 mL.

over the vials, each containing around 20 larvae of *T. castaneum*. The insects were observed for a maximum time point of 36 h. The larvae with colour change and no movement were considered dead. Control groups were maintained under similar conditions without NE beads. Experiments were conducted in triplicates. The numbers of live and dead cells in each vial were counted every 12 h after initial exposure for up to 36 h (12, 24 and 36 h). To evaluate the mortality, the cells were directly observed every hour until total mortality was observed.[36,37]

2.5.3. Determination of ovicidal activity. The development of eggs from adults can be effectively suppressed using NE beads (cinnamon oil nanoemulsion: CNN, clove oil nanoemulsion: CLN, and eugenol nanoemulsion: EGN) with high ovicidal activity. For the experiment, briefly, around 20 eggs of *T. castaneum*, that are roughly 24 h old, were placed in the storage pest control device tubes (Fig. 1). The NE beads were placed in the porous tubes individually, encased within the large tubes. All three NE beads were taken in tested doses and applied on porous tubes. The insects were thus exposed to the test solutions for different time periods (26, 50, 74 and 98 h). After the treatment period, the numbers of dead and live insects were counted and recorded. The percentage of mortality rate was plotted in the graph based on the number of dead insects.[38–41]

2.5.4. Assessment of larvicidal activity. The larvicidal activity was evaluated using the larvae of *T. castaneum* (16 days old) in the presence or absence of wheat flour as the medium. The NE beads (cinnamon oil nanoemulsion: CNN, clove oil nanoemulsion: CLN, and eugenol nanoemulsion: EGN) were taken in the storage pest control device porous tubes (Fig. 1), and the tube is partially closed to check the activity. The insect larvae were exposed to different time periods (24, 48, 72 and 96 h). After each exposure period, the tubes were removed and observed for the mortality of insect larvae. The data mortality counts were subjected to probit analysis.[42,43]

2.6 Statistical analysis

The statistical analyses to determine the activity of the nanoemulsions beads of cinnamon oil nanoemulsion: CNN, clove oil nanoemulsion: CLN, and eugenol nanoemulsion: EGN were performed using two-way ANOVA with the significance of $p \leq 0.05$ at a concentration of LD_{50} of 0.5 g. To eliminate the possibility of inaccuracy, each result was assessed three times. The GraphPad Prism 10 software was used for the computations and graph construction.[44]

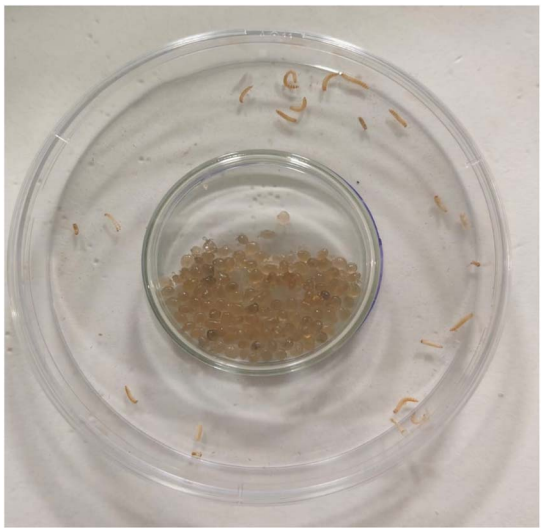

Fig. 2 Repellent activity analysis using a Petri plate.

3. Results and discussion

An essential oil nanoemulsion is crucial for treating red flour beetles, particularly *Tribolium castaneum*, in wheat flour due to their inherent limitations.[19] These emulsions enhance their efficacy and stability, preventing contamination, economic losses, quality deterioration, mold growth, and trade issues.[45] The presence of live beetles can lead to grain rejection and poor feed consumption.[46] To combat these issues, researchers have explored the activity of plant oils as nanoemulsions, using cinnamon, clove, and eugenol essential oils as natural alternatives.[47–49] In this regard, encapsulating the nanoemulsion inside beads (*e.g.*, sodium alginate beads) allows for the slow and sustained release of the active compounds, thereby increasing their efficiency *via* controlled release. This prolongs the insecticidal or repellent action significantly compared to the rapid evaporation or degradation of direct nanoemulsions.[50]

© 2026 The Author(s). Published by the Royal Society of Chemistry

Open Access Article. Published on 06 May 2026. Downloaded on 6/2/2026 7:40:05 AM.
This article is licensed under a Creative Commons Attribution-NonCommercial 3.0 Unported Licence.

Controlled release lowers the overall required dose at any one time, reducing the potential toxicity risks to non-target organisms and the environment.[51] Moreover, nanoemulsion beads offer enhanced insecticidal properties, improved stability, and safety, making them practical for long-term pest management, such as treating red flour beetles in grains. Based on the literature review, we tend to formulate the nanoemulsion beads for the three essential oils, namely cinnamon, clove and eugenol oils, as beads using sodium alginate and calcium chloride.

In order to study their activity against the red flour beetle, particularly *Tribolium castaneum*, we initially formulated nanoemulsion sodium alginate beads using the encapsulation technique and characterized the NE beads using field emission scanning electron microscopy (FESEM) analysis, FT-IR spectroscopy and GC-MS analysis.

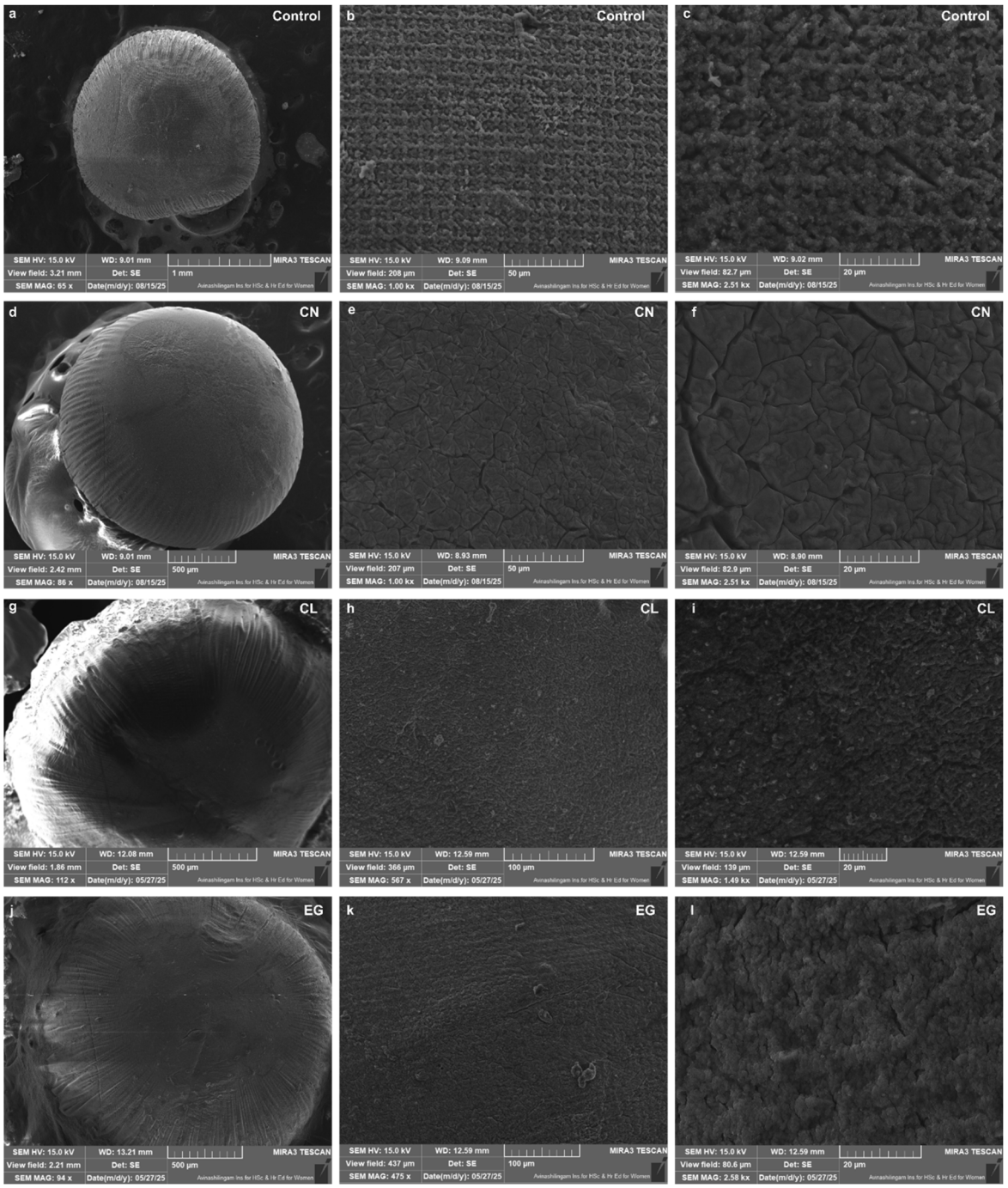

Fig. 3 FESEM images of the sodium alginate beads encapsulating (a–c) sodium alginate beads as control, (d–f) cinnamon oil nanoemulsion beads, (g–i) clove oil nanoemulsion beads, and (j–l) eugenol nanoemulsion beads. All samples exhibit generally spherical- to oval-shaped beads with porous or rough surface morphology, characteristic of the alginate-based encapsulation. Surface features and porosity reflect the influence of formulation parameters and encapsulated oil, supporting effective encapsulation and the potential for controlled release.

© 2026 The Author(s). Published by the Royal Society of Chemistry

Open Access Article. Published on 06 May 2026. Downloaded on 6/2/2026 7:40:05 AM.
This article is licensed under a Creative Commons Attribution-NonCommercial 3.0 Unported Licence.

3.1 Characterization of the nanoemulsion of essential oil beads

3.1.1. Field emission scanning electron microscopy (FESEM) analysis. Field emission scanning electron microscopy (FESEM) analysis was performed to examine the surface morphology and structural characteristics of sodium alginate beads encapsulating cinnamon oil nanoemulsion, clove oil nanoemulsions, and eugenol nanoemulsion. FESEM was also used to characterize nanoemulsion sodium alginate beads by providing the high-resolution images of their surface morphology, size, and structure. These results would reveal the texture of the beads, their size and shape distribution, and their structural integrity.[52] FESEM offers ultra-high resolution at low voltages, minimizing the damage or charging effects on the beads. It also produces a 3D-like image, allowing for detailed visualization of the bead topology.[53] FESEM analysis of all three types of nanoemulsion-loaded alginate beads revealed a generally spherical shape with a porous surface structure, which is typical for alginate-based hydrogel beads prepared by ionic gelation methods. The porosity is influenced by the concentrations of alginate and calcium chloride used during bead formation, with higher concentrations leading to denser beads and smaller pore sizes. This porous morphology facilitates the encapsulation and controlled release of the essential oil. The

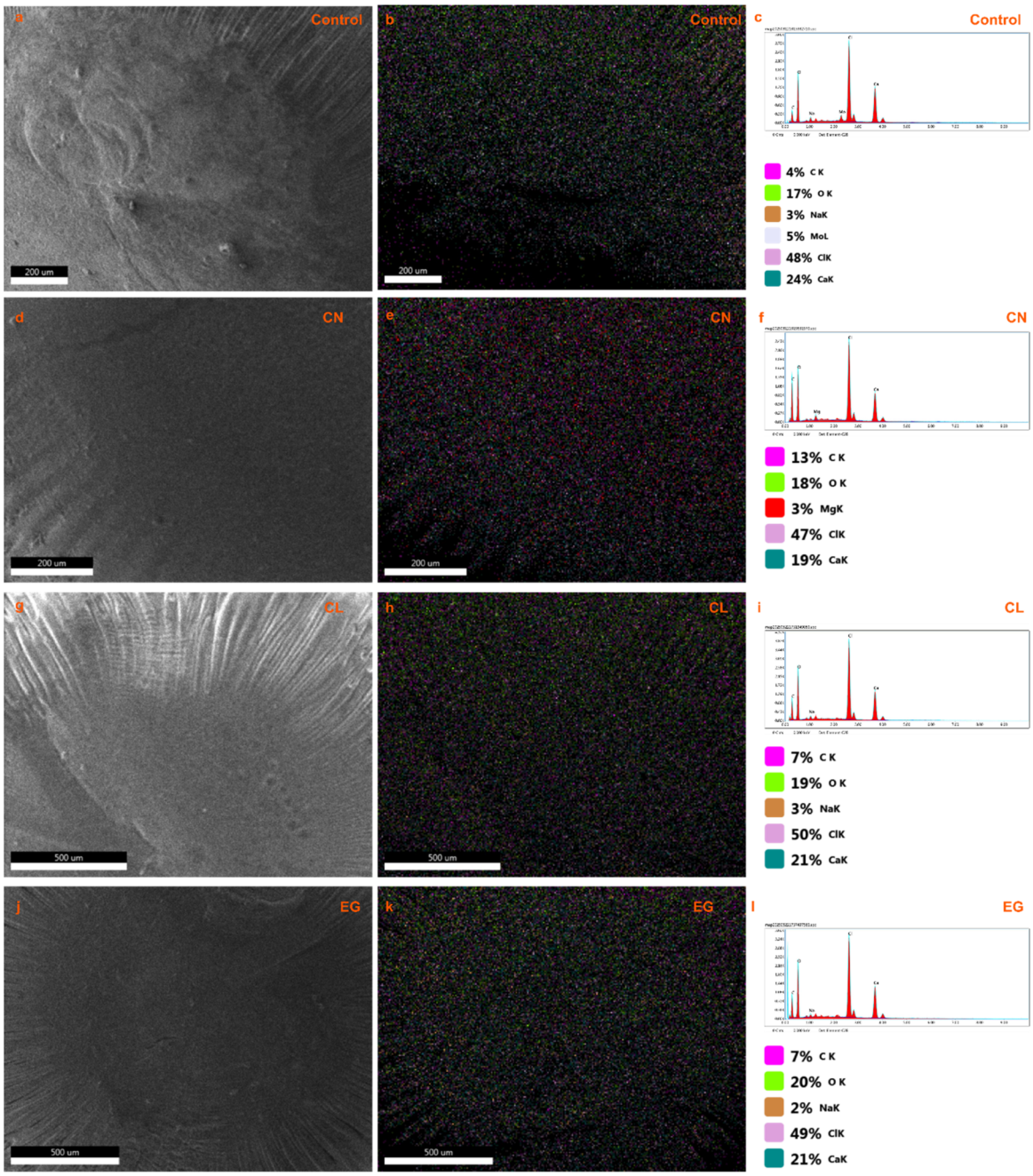

Fig. 4 EDX analysis of the nanoemulsion beads.

© 2026 The Author(s). Published by the Royal Society of Chemistry

Open Access Article. Published on 06 May 2026. Downloaded on 6/2/2026 7:40:05 AM. This article is licensed under a Creative Commons Attribution-NonCommercial 3.0 Unported Licence.

Table 1 Smart quant EDX analysis

NE bead	CK (%)	OK (%)	NaK (%)	MoL (%)	MgK (%)	ClK (%)	CaK (%)
Control	4	17	3	5	—	48	24
CNN	13	18	—	—	3	47	19
CLN	7	19	3	—	—	50	24
EGN	7	20	2	—	—	49	21

bead size was measured using a screw gauge, and the average bead size is 1.34 mm (Fig. 3).

The elemental composition of the NE beads was studied using EDX (energy dispersive X-ray) analysis to identify and quantify the elemental composition. Fig. 4(a–i) shows the intensity of X-rays detected at different energy levels (0.000 keV to 9.00 keV). Each peak in the spectrum corresponds to a specific element present in the sample. The height and area of the peaks are proportional to the concentration of that element. Prominent peaks show the distinct peaks for carbon (C), sodium (Na), calcium (Ca), and chlorine (Cl). The labels "C", "Na", "Ca", and "Cl" are directly associated with their respective peaks, indicating their presence in the sample. These peaks are observed at characteristic energy levels for each element, which helps in their identification. Table 1 represents the quantitative analysis of the elements identified in the spectrum with their concentrations. The identified elements include CK (Carbon K-alpha), OK (Oxygen K-alpha), NoK (Nitrogen K-alpha, though the peak is not explicitly labelled on the graph, it is quantified), ClK (Chlorine K-alpha), and CaK (Calcium K-alpha).

3.1.2. Surface characterization of the nanoemulsion beads. Surface characterization of the NE beads (cinnamon oil nanoemulsion: CNN, clove oil nanoemulsion: CLN, and eugenol nanoemulsion: EGN) was carried out based on the adsorption–desorption isotherms, which are used to characterize the porous structure of materials. *x*-Axis represents the ratio of the equilibrium pressure (P) to the saturation vapor pressure (P_0) of the adsorbate at a given temperature. This indicates the degree of filling of pores. The *y*-axis indicates the volume of gas adsorbed per unit mass of the adsorbent material. This relates to the capacity of the material to adsorb gas. The absorption curve represents the amount of gas adsorbed as the relative pressure increases, while desorption curve shows the amount of gas desorbed as the relative pressure decreases. In terms of hysteresis loop, the separation between the adsorption and desorption curves, particularly evident in graphs in Fig. 5b–d, indicates the presence of mesopores (pores with diameters between 2 and 50 nm). The shape of the hysteresis loop indicates the pore geometry. In some plateau region isotherms (like Fig. 5a and possibly Fig. 5d), a plateau at higher relative pressures suggests the complete filling of pores or multi-layer adsorption. The desorption analysis of the NE beads is shown in Table 2. Surface area ($m^2\ g^{-1}$) indicates the total surface area available per gram of the material. CNN beads show the highest surface area (3.991 $m^2\ g^{-1}$), suggesting a more porous or highly structured material compared to the control (2.947 $m^2\ g^{-1}$) and other beads. EGN beads have the lowest surface area (1.124 $m^2\ g^{-1}$), indicating a less porous structure. In terms of pore volume

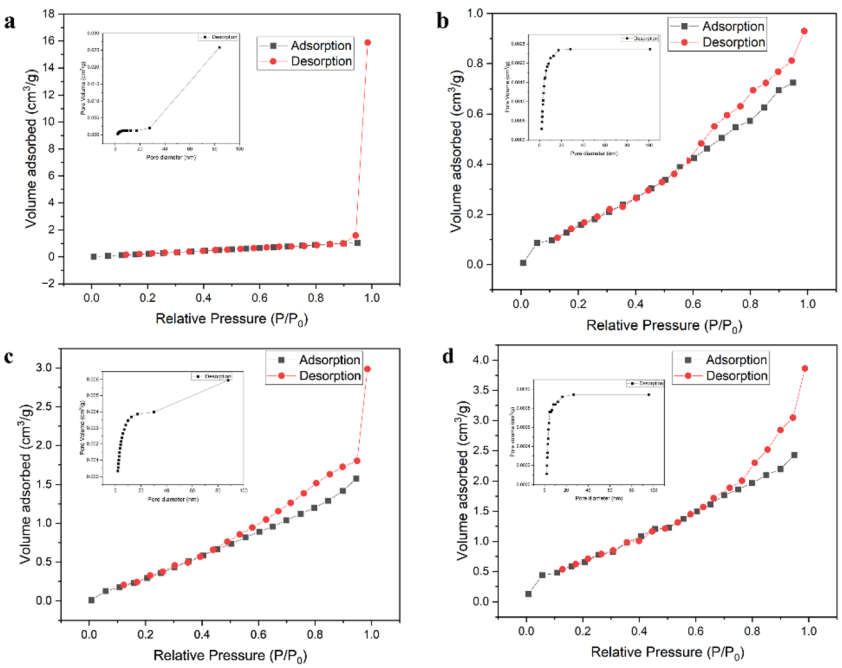

Fig. 5 Absorption–desorption characterization of the NE beads.

Open Access Article. Published on 06 May 2026. Downloaded on 6/2/2026 7:40:05 AM. This article is licensed under a Creative Commons Attribution-NonCommercial 3.0 Unported Licence.

Table 2 Desorption analysis of the nanoemulsion beads

Beads	Surface area (m^2 g^{-1})	Pore volume (cm^3 g^{-1})	Pore diameter DV (d) (nm)
Control	2.947	0.026	2.030
CNN beads	3.991	0.006	2.490
CLN beads	2.581	0.002	2.281
EGN beads	1.124	0.001	2.246

(cm^3 g^{-1}), the total volume of pores within the material per gram is calculated. The control sample has the highest pore volume (0.026 cm^3 g^{-1}), while CLN and EGN beads have significantly lower pore volumes (0.002 cm^3 g^{-1} and 0.001 cm^3 g^{-1}, respectively). This suggests that while CNN beads have a high surface area, their overall pore volume is lower than the control, indicating smaller or less numerous pores despite the increased surface area. The pore diameter DV (d) (nm) represents the average diameter of the pores. The pore diameters are relatively similar across all samples, ranging from 2.030 nm for the control to 2.490 nm for CNN beads, suggesting that while the quantity and surface area of pores vary, the average size of the pores remains within a similar range for these nanoemulsion beads.

FESEM provides high-resolution images of the surface morphology, revealing bead shape, size, texture, and structural features.[54] EDX analysis confirms the elemental makeup, identifying and quantifying elements, and detecting contaminations. This combination helps correlate surface morphology with elemental distribution, crucial for understanding the encapsulation efficiency, stability, and release characteristics. This combination is crucial for optimizing the formulation and functionality in pharmaceutical, cosmetic, or food applications.[55] The elemental composition of NE beads was analysed using EDX (Energy-Dispersive X-ray) analysis. The X-ray detected at different energy levels corresponded to specific elements, with prominent peaks for Carbon, Sodium, Calcium, and Chlorine. The quantitative analysis identified elements like Carbon K-alpha, Oxygen K-alpha, Nitrogen K-alpha, Chlorine K-alpha, and Calcium K-alpha, with their concentrations quantified in Table 1. The surface characterization of NE beads was analysed using adsorption–desorption isotherms to characterize their porous structure. The absorption and desorption curves indicate gas adsorbed and desorbed, respectively. The hysteresis loop, characterized by separation between the two, indicates mesopores with diameters between 2 and 50 nm, particularly evident in Fig. 5b–d, indicating the presence of mesopores which confirms the characteristic of the NEs beads. The desorption analysis of the NEs beads is shown in Table 2. Surface characterization analysis reveals distinct differences in the physical characteristics of the nanoemulsion beads, CNN beads exhibit the largest surface area and pore diameter, while EGN beads have the smallest surface area and pore volume. The control sample, despite having a lower surface area than that of the CNN beads, possesses the highest pore volume (Table 2).

3.1.3. Fourier transform infrared (FTIR) analysis. Cinnamon oil and clove oil are both rich sources of eugenol, and their FTIR spectra closely resemble that of pure eugenol due to the predominance of this compound in their chemical profiles. As shown in Fig. 6, the FTIR spectra of cinnamon oil nanoemulsion beads, clove oil nanoemulsion beads, and eugenol nanoemulsion beads all exhibit the characteristic absorption bands attributable to eugenol. The Fourier Transform Infrared (FTIR) spectra of these essential oil-based nanoemulsions, as well as eugenol nanoemulsion encapsulated in sodium alginate beads, display prominent peaks corresponding to both eugenol and the alginate matrix. The FTIR spectrum of eugenol nanoemulsion beads typically shows strong peaks in the region of 720–1250 cm^{-1}, attributed to C–O and C–H bending and C–O–C stretching vibrations, which serve as a fingerprint for the molecule. Additionally, strong absorption bands appeared at approximately 1512–1637 cm^{-1}, corresponding to the C=C stretching vibrations of the aromatic ring, and a broad band appeared between 3200 and 3600 cm^{-1}, indicative of O–H stretching from the phenolic group. Sodium alginate beads are characterized by a broad O–H stretching band in the 3700–3000 cm^{-1} range, C–H stretching between 3000 and 2850 cm^{-1}, and distinctive carboxylate (COO^-) stretching bands near 1599 cm^{-1} (asymmetric) and 1416 cm^{-1} (symmetric), as well as C–O–C stretching in the 1081–1027 cm^{-1} region. In the FTIR spectra of eugenol-loaded alginate beads, the retention of eugenol's aromatic and ether peaks alongside the characteristic alginate bands confirms the successful encapsulation without significant chemical modification. Minor shifts or changes in peak intensity, particularly in the O–H and C–O–C regions, may suggest physical interactions such as hydrogen bonding between eugenol and the alginate matrix, but no new peaks indicative of strong chemical bonding are typically observed. This spectral profile demonstrates that both eugenol nanoemulsion beads and sodium alginate beads maintain their core structures within the nanoemulsion bead system, with FTIR analysis providing clear evidence of the encapsulation and compatibility of the two components.

The FTIR spectra of control sodium alginate, nano emulsion of bulk oils (of cinnamon, clove, and eugenol) and their NE sodium alginate beads are shown in Fig. 6. The assay was performed to characterize the formulations structurally and functionally to track changes in their structure or functions resulting from interaction with different components upon formulation into nanoemulsions. The presence of looser bands at wavelengths 3000–2800 cm^{-1} in the FTIR spectra for all three emulsions indicate the component stability and better H–OH interactions. This also explains the increased water content in the NE formulation.[56] From Fig. 6, Cinnamon and clove oil are rich sources of eugenol, which is closely resembled in their FTIR spectra due to its predominant presence in their chemical profiles. The FTIR spectra of cinnamon oil nanoemulsion, clove oil nanoemulsion, and eugenol nanoemulsion beads all exhibit the characteristic absorption bands attributable to eugenol. These essential oil-based nanoemulsion beads, as well as eugenol nanoemulsion beads encapsulated in sodium alginate beads, display prominent peaks corresponding to both eugenol and the alginate matrix. Eugenol's strong peaks in the 720–1250 cm^{-1} region, C–O and C–H bending and C–O–C stretching

 © 2026 The Author(s). Published by the Royal Society of Chemistry

Open Access Article. Published on 06 May 2026. Downloaded on 6/2/2026 7:40:05 AM.
This article is licensed under a Creative Commons Attribution-NonCommercial 3.0 Unported Licence.

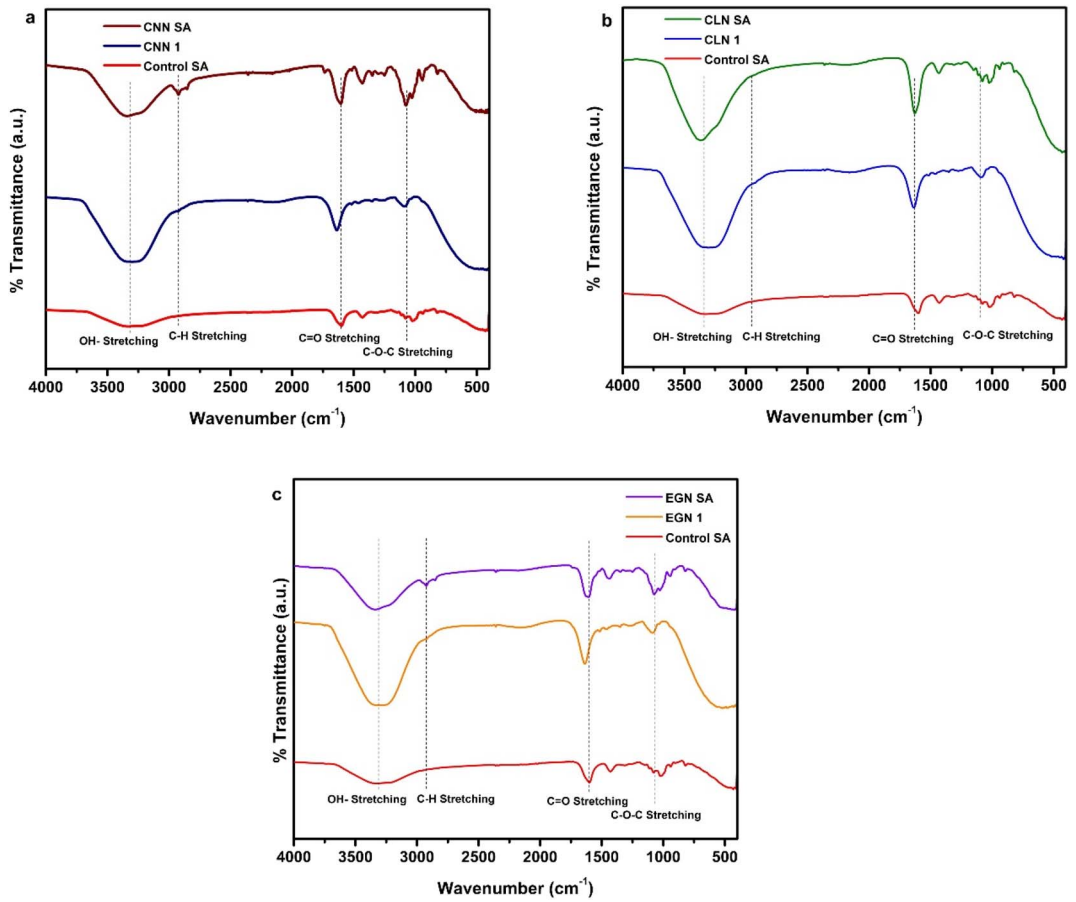

Fig. 6 FTIR spectra of the cinnamon oil nanoemulsion beads (a), clove oil nanoemulsion beads (b), and eugenol nanoemulsion beads (c) encapsulated in sodium alginate beads, showing the characteristic absorption bands of eugenol.

vibrations, serve as a fingerprint for the molecule. Sodium alginate is characterized by broad O–H stretching bands in the 3700–3000 cm^{-1} range, C–H stretching between 3000 and 2850 cm^{-1}, and distinctive carboxylate (COO^{-}) stretching bands near 1599 cm^{-1} (asymmetric) and 1416 cm^{-1} (symmetric). The FTIR spectra of eugenol-loaded alginate beads confirm successful encapsulation without significant chemical modification. Followed by FT-IR analysis, Fig. 7–9 reveal the GC-MS analysis elucidating that eugenol is the only detectable component in all three types of nanoemulsion beads after encapsulation in sodium alginate. This indicates that eugenol is the major volatile compound retained or released from the encapsulated systems, confirming its chemical stability and successful encapsulation. This is crucial for applications involving eugenol as the primary bioactive compound.

3.1.4. GC-MS analysis. The GC-MS (gas chromatography-mass spectrometry) analysis provides a detailed chemical profile of the volatile compounds present in the samples. In this case, the results indicate that eugenol is the sole detectable component in all three types of nanoemulsion beads—cinnamon oil, clove oil, and pure eugenol—after encapsulation in sodium alginate beads. This finding suggests that eugenol is the major or only volatile compound retained or released from the encapsulated systems under the experimental conditions. It also implies that other minor constituents present in the original essential oils are either absent, below the detection limit, or possibly lost during the nanoemulsion preparation and encapsulation processes. The exclusive detection of eugenol in all samples confirms its chemical stability and successful encapsulation, and supports the FTIR results, which also indicate the preservation of eugenol's structural integrity within the sodium alginate matrix. This outcome is particularly relevant for applications where eugenol is the primary bioactive compound of interest, ensuring the efficacy and targeted delivery of the encapsulated product.

Fig. 7(a–c) shows the presence of eugenol in CNN with retention times of 9.29 and 10.10. In CLN, it contains both eugenol and caryophyllene, with retention times spanning 9.11, 9.29, 10.11, 10.57 and 11.38 (Fig. 8(a–d)). EGN primarily contains eugenol, with multiple retention times of 9.02, 9.15, 9.30, and 11.48 (Fig. 9(a–d)). A detailed report of the GC-MS chromatogram is shown in Table S5.

3.2 *In vitro* studies for *Tribolium castaneum* using nanoemulsion essential oil beads

After the characterization of the nanoemulsion sodium alginate beads, *in vitro* assessment of their activity was carried out against *Tribolium castaneum* to check their toxicity based on the

Open Access Article. Published on 06 May 2026. Downloaded on 6/2/2026 7:40:05 AM.
This article is licensed under a Creative Commons Attribution-NonCommercial 3.0 Unported Licence.

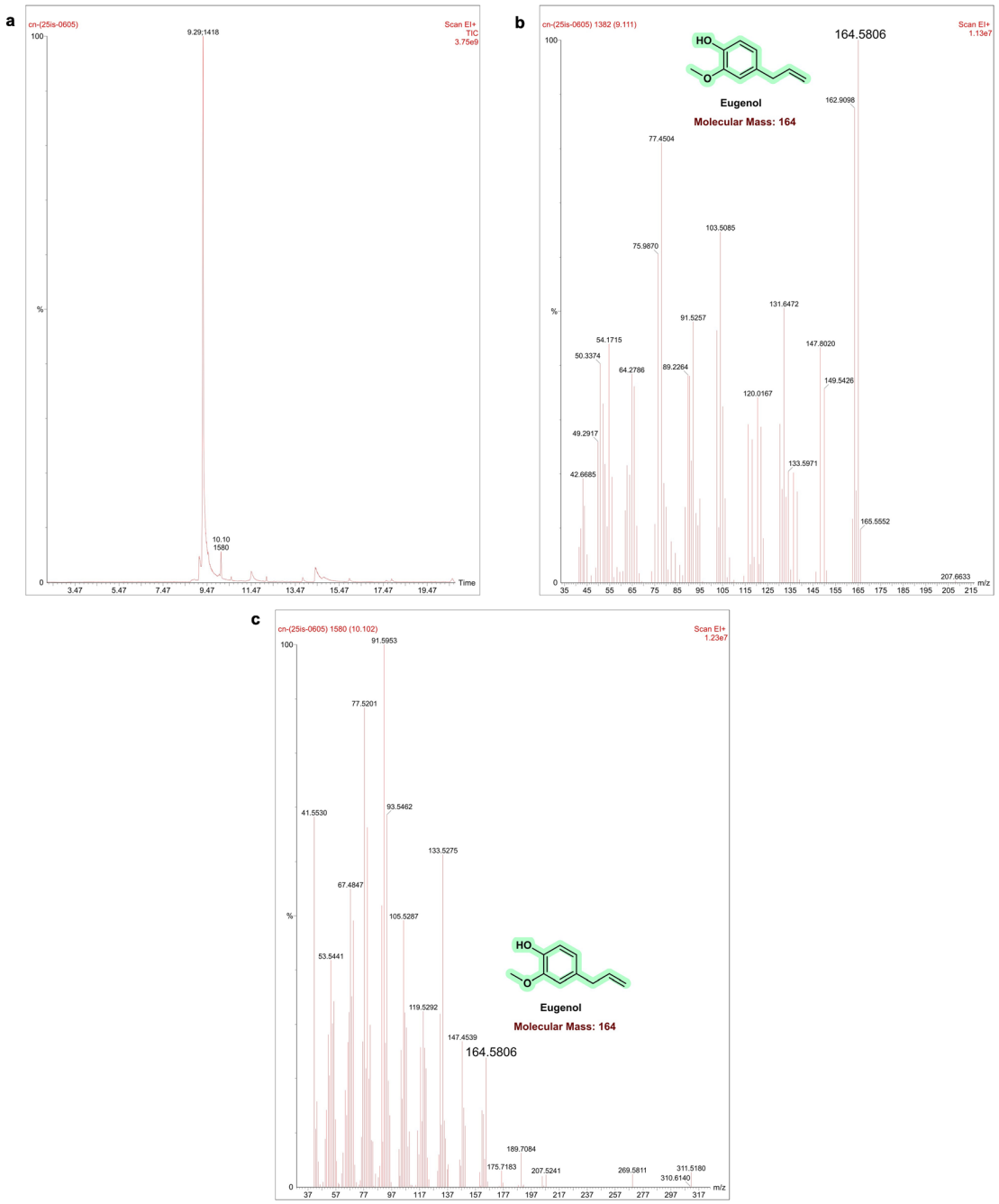

Fig. 7 GC-MS chromatogram and mass spectra of the cinnamon oil nanoemulsions encapsulated in sodium alginate beads.

repellent, fumigant, ovicidal and larvicidal activities. Meanwhile, the release kinetics of the formulated nanoemulsions was studied for about 150 h, and their efficiency is shown in the SI (Fig. S1). Further, the release kinetics of each nanoemulsion bead is shown in Tables S2–S4. Moreover, the lethal concentration of the essential is also optimized, and it is shown in Table S1 in order to confirm their dose effects. Then, the efficacy of the NE beads was compared with the control sodium alginate beads to assess their potential against *Tribolium castaneum*. It is necessary to perform TG-AMS (or at least TGA/TG-MS) on sodium alginate nanoemulsion beads to prove that the carrier system is thermally stable, compositionally well defined, and structurally suitable for controlled diffusion-driven release, rather than just reporting a release curve with unknown underlying material behavior.[57] TGA quantifies the moisture, solvent, and volatile content and identifies degradation temperatures of alginate, drug, and any oil/surfactant components, ensuring that the beads remain intact under processing and storage conditions. In a diffusion study, this confirms that the release profile is not confounded by premature thermal/oxidative degradation or excessive residual volatiles that could plasticize the matrix and alter diffusivity. Multi-step mass-loss

© 2026 The Author(s). Published by the Royal Society of Chemistry

Open Access Article. Published on 06 May 2026. Downloaded on 6/2/2026 7:40:05 AM.
This article is licensed under a Creative Commons Attribution-NonCommercial 3.0 Unported Licence.

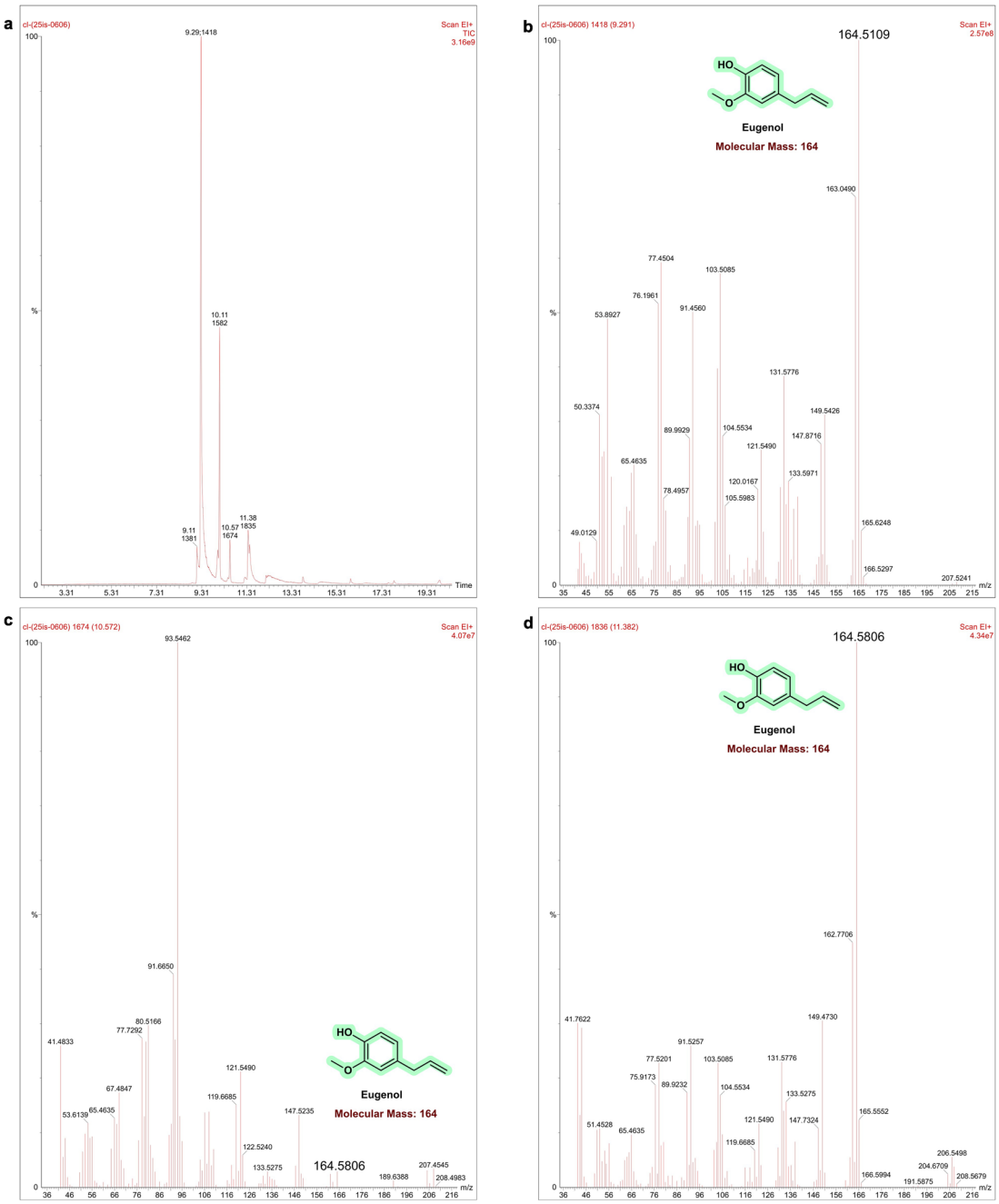

Fig. 8 GC-MS chromatogram and mass spectra of the clove oil nanoemulsions encapsulated in sodium alginate beads.

events and their temperature ranges reflect crosslinking density, bound *vs.* free water, and the presence of additional organic phases; these features help interpret whether the system behaves as a simple Fickian diffuser, a swelling/erosion-controlled system, or a mixed mechanism. The TG-AMS profiles were compared among blank, nanoemulsion-loaded beads and differently crosslinked formulations, the changes in thermal stability and volatile evolution were correlated with fitted release models (*e.g.*, Higuchi, Korsmeyer–Peppas), giving a physicochemical basis for observed diffusion coefficients. Thermal analysis (TGA with DSC or MS) is a standard requirement in preformulation to confirm drug–polymer compatibility, absence of unexpected decomposition products, and overall material integrity, which are critical for regulatory acceptance and reproducible performance of controlled-release beads. For sodium alginate systems in particular, TG-based characterization supports claims about improved stability, controlled release, and robustness of the bead formulation, rather than leaving the mechanism and reliability of diffusion behavior speculative.

3.2.1. Evaluation of repellent activity. Then repellent activity of the NE beads (cinnamon oil nanoemulsion: CNN,

Open Access Article. Published on 06 May 2026. Downloaded on 6/2/2026 7:40:05 AM.
This article is licensed under a Creative Commons Attribution-NonCommercial 3.0 Unported Licence.

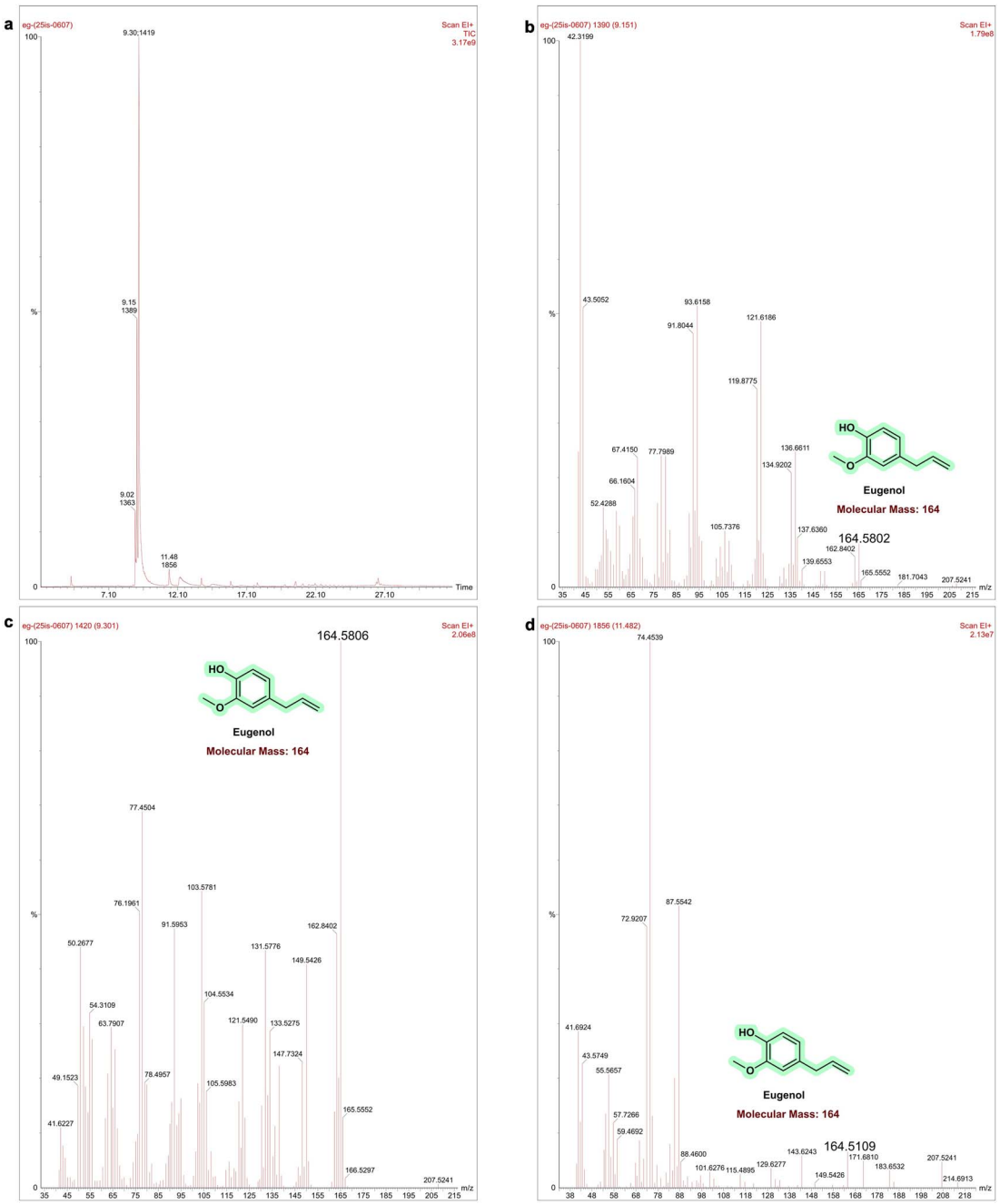

Fig. 9 GC-MS chromatogram and mass spectra of the eugenol nanoemulsions encapsulated in sodium alginate beads. In all panels, eugenol is detected as the predominant and sole volatile compound, confirming its presence and chemical stability following encapsulation. No other major constituents are observed, indicating the specificity and efficiency of the encapsulation process for eugenol.

clove oil nanoemulsion: CLN, and eugenol nanoemulsion: EGN) were tested based on the zone of inhibition. In order to check the repellency activity, we utilized 20 larvae to SA beads and sodium alginate NEs beads of 1 g concentration. Fig. 10 depicts that CNN beads showed the highest repellent activity followed by EGN and CLN beads with a p value less than 0.01, showing its significance. There was no repellancy activity observed in the SA beads.

3.2.2. Evaluation of fumigant activity. In order to check the fumigant activity, larvae were exposed to the fumigants for 12, 24 and 36 h. Insects with no antennal or leg movement were considered dead. Fig. 11 indicates the fumigant activity of the control SA beads and NE beads (cinnamon oil nanoemulsion: CNN, clove oil nanoemulsion: CLN, and eugenol nanoemulsion: EGN), resulting in the highest mortality rate of around 8% at the 36 h by the CNN beads with the statistical significance of $p <$ 0.01. Followed by EGN and CLN beads while this activity was observed in 1 g of concentration of the NEs beads.

3.2.3. Determination of ovicidal activity. The effects of suppressing the development and growth of adults from eggs

© 2026 The Author(s). Published by the Royal Society of Chemistry

Open Access Article. Published on 06 May 2026. Downloaded on 6/2/2026 7:40:05 AM.
This article is licensed under a Creative Commons Attribution-NonCommercial 3.0 Unported Licence.

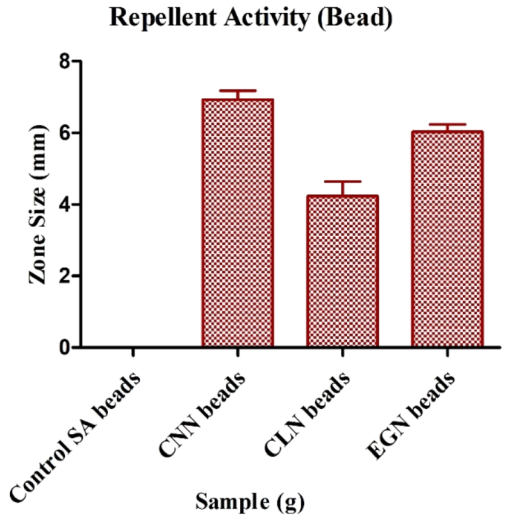

Fig. 10 Repellent activity of SA and NE beads against *T. castaneum* measured based on the zone size.

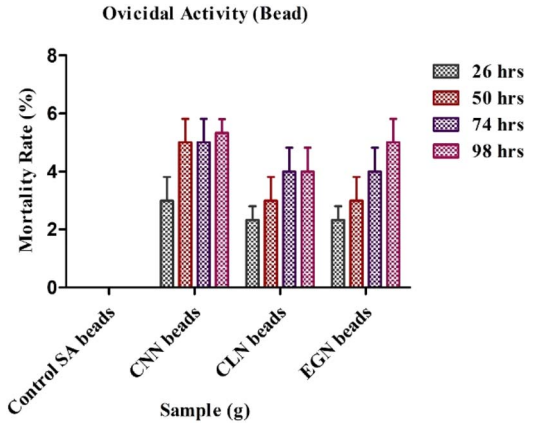

Fig. 12 Ovicidal activity of the SA and NE beads against *T. castaneum* at different time points.

were studied based on the ovicidal activity. The insect larvae were treated with 1 g concentration of NE beads (cinnamon oil nanoemulsion: CNN, clove oil nanoemulsion: CLN, and eugenol nanoemulsion: EGN) for different time periods (26, 50, 74 and 98 h), and the toxicity was observed parallelly with the increasing time of exposure. Fig. 12 explains the ovicidal activity of the NE beads at different time points and measured based on the mortality rate. From this analysis, CNN beads showed the highest mortality rate at 98 h time point, followed by EGN and CLN beads with a significant p value less than 0.01. However, the SA beads do not show any ovicidal activity, indicating its non-effective nature against the eggs.

3.2.4. Assessment of larvicidal activity. The larvicidal activity of the sodium alginate and the NE beads (cinnamon oil nanoemulsion: CNN, clove oil nanoemulsion: CLN, and eugenol nanoemulsion: EGN) was tested at different time points up to 30 h. The mortality rate of *T. castaneum* larvae was observed and Fig. 13 shows CNN beads have achieved larvicidal activity at maximum time point of 30 h. From this analysis, it is known that the larvicidal activity increases proportionally with the increase in the time of exposure. CNN beads showed higher mortality rate, followed by EGN and CLN while control SA beads showed no activity indicating its non-toxic nature including $p < 0.01$. Moreover, it shows null effect on the insects.

Meanwhile, in all the *in vitro* assessments, the control sodium alginate beads showed no effect, indicating that its presence does not impact the *Tribolium castaneum*. Based on the results of *in vitro* assessments, it is evident that the CNN NEs beads has significant effect on the treating *Tribolium castaneum*, also proving the formulated NEs beads with sodium alginate doesn't infer in the any toxic effect against the insects. Because of its smaller droplet size and greater dispersion, the nanoemulsion of cinnamon oil is extremely poisonous to storage pests like *Tribolium castaneum*, resulting in increased fatality rates at lower concentrations.[6,58] On the other hand, eugenol oil nanoemulsion is thought to be a viable ovicidal agent for integrated pest management in stored grains due to its improved insecticidal characteristics. Although most of the published research concentrate on adulticidal activity, ovicidal effects they are deduced from the enhanced overall toxicity profile. Its nano-

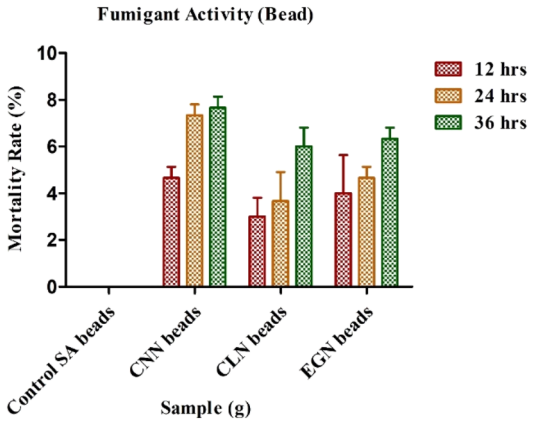

Fig. 11 Fumigant activity of the SA and NE beads against *T. castaneum* measured based on the mortality rate.

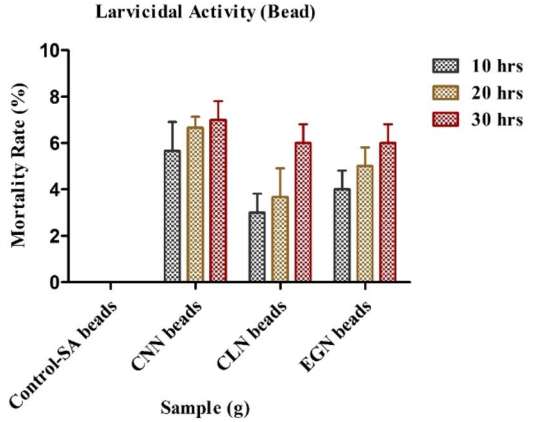

Fig. 13 Larvicidal activity of the SA and NE beads against *T. castaneum* at different time points.

Open Access Article. Published on 06 May 2026. Downloaded on 6/2/2026 7:40:05 AM. This article is licensed under a Creative Commons Attribution-NonCommercial 3.0 Unported Licence.

formulation increases penetration and efficacy, making it more effective than the standard eugenol oil.[36,59]

4. Conclusion

In this study, we demonstrated that nanoemulsion bead formulations using cinnamon, clove, and eugenol exhibit strong pesticidal potential against *Tribolium castaneum*, a major pest of stored grains. The enhanced stability, bioavailability, and sustained release of active compounds in the nanoemulsion form significantly improved their efficacy compared to conventional formulations. In our study, among the formulated NE beads, CNN NEs beads have significant effect on the treating *Tribolium castaneum*, also proving the formulated NEs beads with sodium alginate doesn't infer in the any toxic effect against the insects. Because of its smaller droplet size and greater dispersion, the nanoemulsion of cinnamon oil is extremely poisonous to storage pests, showed the highest mortality and repellency, suggesting its promise as a potent eco-friendly bioinsecticide. These findings highlight the potential of essential oil-based nanoemulsion beads as sustainable alternatives to synthetic pesticides, offering effective pest management while minimizing environmental and health risks. Limitations of this study includes the efficacy of the NE bead has been tested in only one pest others remain untested. Moreover, in future, the study needs to be extended to the other food pests and gender-wise experiments, and biodegradability also needs to be investigated. However, comprehensive ecotoxicological assessments, including impacts on non-target organisms such as pollinators, natural predators, and soil microbes, were not performed, which remains an important next step.

Ethics statement

The study utilized a novel biopolymer-based biopesticide patented under appropriate licensing agreements and in compliance with the institutional and international intellectual property regulations. Patent number for biopolymer-based biopesticide: 202541021057. The study utilized novel bead encapsulator patented instruments under appropriate licensing agreements and in compliance with the institutional and international intellectual property regulations. Patent number for bead encapsulator: 202541021001. Moreover, we utilized the novel storage pest control device which is under consideration of the patent under the applicant name of Vellore Institute of Technology, Vellore.

Author contributions

Nagarathinam Kannan: writing – review and editing, writing – original draft, visualization, validation, methodology, investigation, formal analysis, and data curation. Dr Natarajan Chandrasekaran: writing – review and editing, visualization, validation, supervision, resources, project administration, methodology, funding acquisition, formal analysis, data curation, and writing – conceptualization.

Conflicts of interest

There are no conflicts to declare.

Data availability

The data will be made available upon request.

Supplementary information (SI) is available. See DOI: https://doi.org/10.1039/d6ra02377k.

Acknowledgements

The authors greatly acknowledge the All India Council for Technical Education for the financial support through the research grant File No.-P/11/2024-US C1/1 (patent has been published number 202641010446).

References

1 P. R. Kale, V. S. Pawar and S. N. Shendge, *Pharma Innovation*, 2021, **10**, 667–673.
2 J. Fornal, T. Jeliński, J. Sadowska, S. Grundas, J. Nawrot, A. Niewiada, J. R. Warchalewski and W. Błaszczak, *J. Stored Prod. Res.*, 2007, **43**, 142–148.
3 R. P. Haff and D. C. Slaughter, *Trans. Am. Soc. Agric. Eng.*, 2004, **47**, 531–537.
4 S. T. N. Nova, J. Mahboba, A. M. Alim and B. K. Mandal, Management of the red flour beetle Tribolium castaneum in stored wheat using dry dust of Neem, *J. Entomol. Zool. Stud.*, 2020, **8**, 1993–2000.
5 G. C. Sekar, K. I. Singh, R. Loganathan and O. Singh, *Agric. Sci. Dig.*, 2025, **45**, 144–147.
6 M. I. Ullah, K. Akram, A. B. M. Raza, M. Arshad, S. Khalid, H. Latif, A. Amjad, N. Perveen and E. Sajid, *Punjab Univ. J. Zool.*, 2024, **39**, 61–67.
7 R. Sharmin, S. Haque, M. J. F. Rumpa and S. I. Faruki, *Asian J. Res. Zool.*, 2024, **7**, 125–132.
8 T. A. Wagan, W. Wang, H. Hua, L. Rong-Hua and W. Cai, *Fla. Entomol.*, 2022, **105**, 160–166.
9 M. J. G. Fernandes, R. B. Pereira, D. M. Pereira, A. G. Fortes, E. M. S. Castanheira and M. S. T. Gonçalves, *Int. J. Mol. Sci.*, 2020, **21**, 9257.
10 S. Koch, A. Epp, M. Lohmann and G. F. Böl, *J. Food Prot.*, 2017, **80**, 2083–2089.
11 H. Omidian, L. X. Cubeddu and E. J. Gill, *Molecules*, 2025, **30**, 520.
12 Preeti, S. Sambhakar, R. Malik, S. Bhatia, A. Al Harrasi, C. Rani, R. Saharan, S. Kumar, Geeta and R. Sehrawat, *Scientifica*, 2023, DOI: 10.1155/2023/6640103.
13 N. G. Kavallieratos, A. Skourti, E. P. Nika, C. T. Ntalaka, M. C. Boukouvala, G. Bonacucina, M. Cespi, R. Petrelli, L. Cappellacci, F. Maggi, G. Benelli and A. Canale, *J. Stored Prod. Res.*, 2021, DOI: 10.1016/j.jspr.2021.101859.
14 T. Riaz, S. Abid, M. Afzal and F. R. Shakoori, *J. Stored Prod. Res.*, 2025, DOI: 10.1016/j.jspr.2025.102579.
15 K. A. Draz, R. M. T. Icon, M. I. Eldosouky and A. A. D. M. Abdelnasser, *Int. J. Pest Manage.*, 2022, 729–743.

© 2026 The Author(s). Published by the Royal Society of Chemistry

Open Access Article. Published on 06 May 2026. Downloaded on 6/2/2026 7:40:05 AM. This article is licensed under a Creative Commons Attribution-NonCommercial 3.0 Unported Licence.

16 A. Hashem and M. Ramadan, *J. Plant Prot. Pathol.*, 2021, **12**, 11–17.
17 M. M. Adel, M. A. Massoud, M. I. Mohamed, K. H. Abdel-Rheim and S. S. Abd El- Naby, *Adv. Crop Sci. Technol.*, 2018, **06**, 1–7.
18 L. Z. Iqbal, F. Ikhtiar, M. U. Farooq, M. F. Faraz, T. Riaz, A. Haider and R. H. Ullah, *Brazilian Journal of Science*, 2025, **4**, 1–24.
19 A. S. Hashem, S. S. Awadalla, G. M. Zayed, F. Maggi and G. Benelli, *Environ. Sci. Pollut. Res.*, 2018, **25**, 18802–18812.
20 I. Zibaee, J. M. Razi, M. H. Farahani and M. N. Moghaddan, *J. Entomol. Zool. Stud.*, 2016, **4**, 80–85.
21 N. Jose, D. P. Ray, S. Misra, L. Nayak and L. Ammayappan, *J. Stored Prod. Res.*, 2024, **109**, 102468.
22 M. Kostyukovsky, E. Quinn, G. Golden, A. Rapaport, E. Shaaya and E. Poverenov, *12th Int. Work. Conf. Stored Prod. Prot. Berlin, Ger., 7–11 Oct., 2018*, 2018, pp. 458–462.
23 P. Jasrotia, M. Nagpal, C. N. Mishra, A. K. Sharma, S. Kumar, U. Kamble, A. K. Bhardwaj, P. L. Kashyap, S. Kumar and G. P. Singh, *Front. Nanotechnol.*, 2022, **3**, 1–19.
24 R. Goodman, *J. Insect Sci.*, 2012, **12**, 1–10.
25 A. Sokoloff, *The Biology of Tribolium casteneum*, Oxford Univ. Press, 1975.
26 M. Deb and D. Kumar, *Entomon*, 2021, **46**, 81–86.
27 K. Adhikari, B. Khanikor and R. Sarma, *Sci. Rep.*, 2022, **12**, 1–11.
28 S. Singh and S. Prakash, *International Journal of Scientific and Research Publications*, 2015, **5**, 2250–3153.
29 T. S. de Oliveira, A. M. M. Costa, L. M. C. Cabral, O. Freitas-Silva and R. V. Tonon, *Int. J. Biol. Macromol.*, 2024, DOI: 10.1016/j.ijbiomac.2024.133627.
30 Z. Zainal-Abidin, *Open Conf. Proc. J.*, 2014, **4**, 12–16.
31 A. Valizadeh, M. Shirzad, F. Esmaeili and A. Amani, *Nanomed. Res. J.*, 2018, **3**, 37–43.
32 M. Paul, S. G. Kang, J. Im and W. J. Song, *Sci. Rep.*, 2024, **14**, 1–14.
33 Y. N. Ashagrie, M. G. Tadesse and R. K. Bachheti, *Sci. Rep.*, 2025, 1–17.
34 M. M. A. Sabbour, *Bull. Natl. Res. Cent.*, 2020, DOI: 10.1186/s42269-020-00336-6.
35 M. Mondal and M. Khalequzzaman, *J. Biosci.*, 2014, DOI: 10.3329/jbs.v17i0.7102.
36 S. S. Ibrahim, U. Sahu, P. Karthik and S. E. Vendan, *J. Food Sci. Technol.*, 2023, **60**, 1435–1445.
37 M. J. Ara, J. A. Khanam, M. Rakibuzzaman and A. F. M. J. Uddin, *J. Biosci. Agric. Res.*, 2019, **21**, 1762–1766.
38 H. M. Kamran, Mansoor-Ul-Hasan, M. Sagheer, A. A. Khan, H. M. Aatif, M. Ijaz, C. M. S. Hanif and S. K. Abbas, *Z. Arznei- Gewuerzpflanzen*, 2017, **22**, 14–19.
39 S. Firooziyan, A. Amani, M. Osanloo, S. H. Moosa-Kazemi, H. R. Basseri, H. M. Hajipirloo, A. Sadaghianifar and M. M. Sedaghat, *J. Environ. Health Sci. Eng.*, 2021, **19**, 1025–1034.
40 C. G. Faustino, F. A. de Medeiros, A. K. R. Galardo, A. B. L. Rodrigues, R. L. Martins, Y. d. M. S. Lima, J. F. Tavares, M. A. A. de Medeiros, J. D. S. Cruz and S. S. M. d. S. de Almeida, *Molecules*, 2020, DOI: 10.3390/molecules25225333.
41 H. Motulsky, *Analyzing Data with GraphPad Prism*, 1999.
42 M. A. Al Bachchu, K. Ara, M. N. Uddin and R. Ara, *Journal of the Asiatic Society of Bangladesh, Science*, 2017, **43**, 223–232.
43 T. O. Nicolescu, *Mass Spectrom.*, 2017, DOI: 10.5772/intechopen.68595.
44 H. M. McNair and J. M. Miller, *J. Am. Chem. Soc.*, 1998, DOI: 10.1021/ja9856001.
45 E. S. M. Elnabawy, S. Hassan and E. K. A. Taha, *Biology*, 2022, **11**, 1–9.
46 G. C. Sekar, K. I. Singh, N. Nagaraju, N. O. Singh and L. N. Singh, *Int. J. Agric. Environ. Biotechnol.*, 2021, **14**, 381–386.
47 P. A. Bordoloi, P. Rajkumari, N. Borah and K. Borah, *International Journal of Advanced Biochemistry Research*, 2024, **8**, 1284–1289.
48 J. Kowalska, J. Tyburski, K. Matysiak, M. Jakubowska, J. Łukaszyk and J. Krzymińska, *Molecules*, 2021, **26**, 1–13.
49 J. P. Boito, A. S. Da Silva, J. H. dos Reis, D. S. Santos, R. R. Gebert, A. H. Biazus, R. C. V. Santos, P. M. Quatrin, A. F. Ourique, A. A. Boligon, D. Baretta, M. D. Baldissera, L. M. Stefani and G. Machado, *Rev. MVZ Cordoba*, 2018, **23**, 6628–6636.
50 E. Ee, M. H. Rady, S. Aa Mo'men, S. Am Ma'moun and M. S. Salama, *Int. J. Mosq. Res.*, 2019, **6**, 63–69.
51 I. F. Mustafa and M. Z. Hussein, *Nanomaterials*, 2020, **10**, 1–26.
52 R. P. Jaya, in *New Materials in Civil Engineering*, Elsevier, 2020, pp. 493–527.
53 R. Senthil Prabhu, R. Priyanka, M. Vijay and G. R. Kaviya Vikashini, *Int. J. Pharm. Biol. Sci.*, 2021, **11**, 2321–3272.
54 R. Lamba, *Biomass Convers. Biorefin.*, 2023, 12157–12166.
55 H. Soonmin, *International Journal of Thin Film Science and Technology*, 2022, **11**, 1–9.
56 N. Chandrasekaran, G. Priya and C. Doss, *RSC Med. Chem.*, 2023, **14**, 433–443.
57 M. H. Ghafariyan, M. J. Malakouti, M. R. Dadpour, P. Stroeve and M. Mahmoudi, *Environ. Sci. Technol.*, 2013, **47**, 10645–10652.
58 R. G. Attia, M. M. H. Khalil, M. A. Hussein, H. M. A. Fattah, S. A. Rizk and S. A. M. Ma'moun, *Neotrop. Entomol.*, 2023, **52**, 500–511.
59 M. N. Wahba, E. A. Abdelatef and T. F. Wahba, *Middle East J. Appl. Sci.*, 2022, **12**, 532–543.